

# Optical spin injection in graphene with Rashba spin-orbit interaction

M. Ingot,<sup>1</sup> V. K. Dugaev,<sup>1,2</sup> E. Ya. Sherman,<sup>3,4</sup> and J. Barnaś<sup>5,6</sup>

<sup>1</sup>*Department of Physics, Rzeszów University of Technology,  
ul. Powstańców Warszawy 6, 35-959 Rzeszów, Poland*

<sup>2</sup>*Departamento de Física and CFIF, Instituto Superior Técnico,  
Universidade de Lisboa, av. Rovisco Pais, 1049-001 Lisbon, Portugal*

<sup>3</sup>*Department of Physical Chemistry, Universidad del País Vasco UPV-EHU, 48080 Bilbao, Spain*

<sup>4</sup>*IKERBASQUE Basque Foundation for Science, Bilbao, Spain*

<sup>5</sup>*Faculty of Physics, Adam Mickiewicz University, ul. Umultowska 85, 61-614 Poznań, Poland*

<sup>6</sup>*Institute of Molecular Physics, Polish Academy of Sciences,  
ul. M. Smoluchowskiego 17, 60-179 Poznań, Poland*

(Dated: March 26, 2014)

We calculate the efficiency of infrared optical spin injection in single-layer graphene with Rashba spin-orbit coupling and for in-plane magnetic field. The injection rate in the photon frequency range corresponding to the Rashba splitting is shown to be proportional to the ratio of the Zeeman and Rashba splittings. As a result, large spin polarization can be controllably achieved for experimentally available values of the spin-orbit coupling and in magnetic fields below 10 Tesla.

PACS numbers: 72.25.Fe, 78.67.Wj, 81.05.ue, 85.75.-d

## I. INTRODUCTION

Graphene – a two-dimensional hexagonal lattice of carbon atoms – was discovered about eight years ago<sup>1-3</sup> and is now one of the most promising materials for future nanoelectronics. The high application potential of this novel material is associated with some peculiarities of its electronic and phonon transport properties<sup>4</sup> as well as with its outstanding mechanical<sup>5,6</sup> and optical properties<sup>7</sup>. Optoelectronic properties of graphene are also very promising for applications<sup>8</sup>. Moreover, owing to a very long spin relaxation time, which is expected due to a very weak spin-orbit interaction, graphene is also attractive for applications in spin electronics (see, e.g., Ref. [9]).

However, to utilize the outstanding properties of graphene for spin-dependent transport, one needs to have a reliable method of controllable spin injection and spin manipulation. The possibility of a relatively strong Rashba spin-orbit coupling has been reported in Refs. [10,11] for graphene deposited on a Ni (or Ni/Au) substrate. Such a strong spin-orbit coupling formally enables spin manipulation in graphene. However, even in the absence of a substrate leading to strong spin-orbit coupling, experiments report spin relaxation time on the timescale of the order of or less than one nanosecond<sup>12-14</sup>, which makes applications of graphene in spin electronics rather difficult. In all the experiments aimed at the measurements of spin relaxation time, spins are injected *en masse* from a ferromagnetic contact giving rise to some charge/spin density distribution, which influences its subsequent dynamics. Several theoretical approaches (see for example Refs. [15–19]) have been proposed to describe spin relaxation. However, most of them demonstrated spin relaxation time much longer than that observed experimentally.

There are several experimental techniques which can

be used to manipulate and control electron spin in graphene. For example, spin current and spin density in graphene nanodisks can be manipulated by varying length of the corresponding zigzag edge<sup>20</sup>. Quantum pumping of Dirac fermions and spin current in a monolayer graphene in perpendicular magnetic field, with the gate voltage as a control parameter, has been proposed in Ref. [21]. Furthermore, the method of spin current generation in a monolayer graphene through adiabatic quantum pumping by two oscillating in time potentials has been described in Refs. [22,23] and for the bilayer graphene in Ref. [24].

It is well-known that spin-orbit coupling can lead to a direct optical spin injection – the technique extensively used in the physics of semiconductors<sup>25</sup>. For graphene, the spin-orbit coupling influences the optical response in the infrared frequency range<sup>26</sup>. In this paper we consider the infrared optical spin injection in a single-layer graphene by linearly polarized light. The graphene is assumed to be deposited on a substrate which leads to the Rashba spin-orbit coupling. Due to this interaction, the electronic spectrum of graphene near the Dirac points splits into four bands with parabolic dependence on the electron momentum at small wave vectors and linear dispersion at large wave vectors<sup>27</sup>. Splitting of the subbands is determined by the spin-orbit coupling strength. We show that optical spin injection becomes allowed in the presence of an external magnetic field, and the injection efficiency is of the order of the ratio of the Zeeman splitting and the spin-orbit coupling matrix element. By modifying the infrared light frequency, one can change the absorption region in the momentum space, and thus control the spin injection.

In Sec. 2 we derive some general formula for optical spin injection efficiency in graphene. Numerical results on spin injection rate are presented and described in Sec. 3. Summary and final conclusions are in Sec. 4.

## II. SPIN INJECTION RATE AND EFFICIENCY

We assume an external magnetic field  $\mathbf{B}$  oriented in the graphene plane. Hamiltonian describing the low energy electron excitations near the Dirac point  $K$  in graphene with the Rashba spin-orbit interaction takes then the form<sup>28</sup>

$$\hat{H} = v(\boldsymbol{\tau} \cdot \mathbf{k}) + g(\mathbf{B} \cdot \boldsymbol{\sigma}) + \lambda(\tau_x \sigma_y - \tau_y \sigma_x), \quad (1)$$

where  $g = g_L \mu_B / 2$ ,  $\lambda = \alpha / 2$  with  $\alpha$  being the coupling constant of Rashba spin-orbit interaction,<sup>27</sup> and  $g_L$  is the Landé factor. The matrices  $\boldsymbol{\tau}$  and  $\boldsymbol{\sigma}$  are the Pauli matrices in the sublattice and spin space, respectively. The third term of the above Hamiltonian stands for the Rashba spin-orbit coupling induced by the substrate. Note, the first term is diagonal in the spin space and for abbreviation the corresponding unit matrix is not written explicitly. Similarly, the second term is diagonal in the sublattice space and the corresponding unit matrix is not written explicitly, too.

Electronic spectrum corresponding to the Hamiltonian (1) consists of four energy bands. In the limit of weak magnetic field,  $gB/\lambda \rightarrow 0$ , this spectrum is described by the formulas

$$E_{n\mathbf{k}}^{(0)} = \pm \lambda \pm (\lambda^2 + v^2 k^2)^{1/2}, \quad (2)$$

with all possible combination of the  $+$  and  $-$  signs, and the index  $n$  labeling the bands in the order of increasing energy (see Fig. 1).

As in the usual two-dimensional electron gas with Rashba spin-orbit interaction, the expectation value of the spin  $z$ -component in eigenstates of Hamiltonian (1) for  $B = 0$  is equal to zero. However, unlike to the two-dimensional electron gas, the expectation value of the in-plane spin depends on the wave vector and is relatively small for low-energy electron states. Indeed, the expectation value,  $\langle \Psi_{n\mathbf{k}}^{(0)} | \boldsymbol{\sigma} | \Psi_{n\mathbf{k}}^{(0)} \rangle$ , of electron spin in the state  $\Psi_{n\mathbf{k}}^{(0)}$  for  $B = 0$  is given by<sup>27</sup>

$$\mathbf{s} \equiv \langle \Psi_{n\mathbf{k}}^{(0)} | \boldsymbol{\sigma} | \Psi_{n\mathbf{k}}^{(0)} \rangle = \frac{\xi v (\mathbf{k} \times \hat{\mathbf{z}})}{\sqrt{\lambda^2 + v^2 k^2}}, \quad (3)$$

where  $\xi = \pm 1$  is the band index,  $\xi = 1$  for  $n = 2, 3$  and  $\xi = -1$  for  $n = 1, 4$  (cf. Ref. [27]). Thus, when  $vk \ll \lambda$ , the expectation value of spin is small,  $|\mathbf{s}| \ll 1$ . Moreover, the spins are perpendicular to the wave vectors, similarly as in two-dimensional electron gas. We note that the upper index (0) at the eigenfunctions and eigenenergies indicates they are for  $B = 0$ .

In the following, we take the in-plane magnetic field  $\mathbf{B}$  along the  $x$ -axis and assume it is rather weak,  $gB/\lambda \ll 1$ . The former assumptions justifies the absence of Landau quantization, while the latter condition assures that the band dispersion is only weakly perturbed by the static magnetic field, and the resulting spin injection is linear in the applied magnetic field  $\mathbf{B}$ . The four-band structure is presented in Fig. 1, which also shows the assumed position of the Fermi level  $\mu$ .

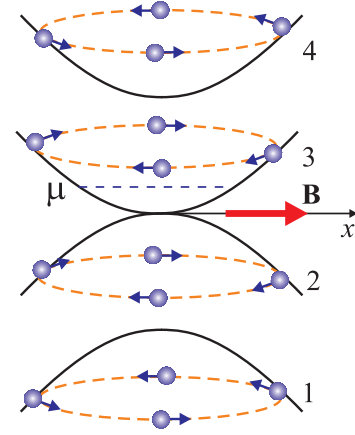


FIG. 1: (Color online). Band structure of graphene with a Rashba spin-orbit interaction in the  $gB/\lambda \ll 1$  limit. Arrows show the  $\mathbf{k}$ -dependent orientation of electron spins in the eigenstates of the Hamiltonian. Here we consider only the vicinity of the  $K$  Dirac point, taking into account that the other valley gives exactly the same result for light absorption and spin injection.

Taking into account the first term of Eq. (1), Hamiltonian describing interaction of graphene with an external periodic electromagnetic field  $\mathbf{A}(t) = \mathbf{A}_0 e^{-i\omega t}$  can be written as

$$\hat{H}_A = -\frac{ev}{\hbar c} (\boldsymbol{\tau} \cdot \mathbf{A}). \quad (4)$$

This periodic perturbation leads to electron transitions between the bands shown in Fig. 1. The spin states of electrons involved in the transitions are then modified accordingly. Without loss of generality, we assume in the following that the electromagnetic field is oriented along the  $y$ -axis,  $\mathbf{A}_0 = (0, A_0, 0)$ .

The total absorption rate of photons can be calculated as the sum of all allowed transitions,

$$I(\omega) = \sum_{nn'} I^{n \rightarrow n'}(\omega), \quad (5)$$

where  $I^{n \rightarrow n'}(\omega)$  corresponds to the absorption associated with the transitions of electrons from the subband  $n$  to the subband  $n'$ , which can be calculated from the Fermi golden rule as

$$I^{n \rightarrow n'}(\omega) = \frac{2\pi}{\hbar} \int \frac{d^2 \mathbf{k}}{(2\pi)^2} \left| \langle \Psi_{n\mathbf{k}} | \hat{H}_A | \Psi_{n'\mathbf{k}} \rangle \right|^2 \times \delta(E_{n\mathbf{k}} + \hbar\omega - E_{n'\mathbf{k}}) f(E_{n\mathbf{k}}) [1 - f(E_{n'\mathbf{k}})]. \quad (6)$$

Here,  $\Psi_{n\mathbf{k}}$  and  $E_{n\mathbf{k}}$  are the eigenfunctions and eigenvalues of the total Hamiltonian (1), and  $f(E_{n\mathbf{k}})$  is the corresponding Fermi distribution function.

It is convenient to introduce an independent of the system parameter  $I_0$ , defined as

$$I_0 = \frac{\omega}{4} \left( \frac{e}{\hbar c} \right)^2 A_0^2, \quad (7)$$

and rewrite Eq. (5) as

$$I(\omega) = I_0 \sum_{nn'} \tilde{I}^{n \rightarrow n'}(\omega) \equiv I_0 \tilde{I}(\omega), \quad (8)$$

with the system-dependent functions  $\tilde{I}^{n \rightarrow n'}(\omega)$ . Since  $A_0^2$  in Eq. (7) is related to the incident flux  $q$  of  $y$ -polarized photons by the formula  $A_0^2 = 4\pi\hbar c q/\omega$ , Eq. (7) can be presented in the form

$$I_0 = \frac{\pi e^2}{\hbar c} q. \quad (9)$$

The ratio  $I_0/q = \pi e^2/\hbar c$  corresponds to the absorption coefficient of graphene without Rashba spin-orbit coupling.<sup>3,29,30</sup> In the limit of large frequency,  $\hbar\omega \gg \lambda$ , the absorption rate (8) is constant and does not depend on frequency, like in the case of graphene with zero Rashba coupling,  $I(\omega) \rightarrow I_0$ . Thus,  $\tilde{I}(\omega)$  can be considered as a ratio of absorption coefficients for graphene with Rashba spin-orbit interaction and of graphene without Rashba interaction. In other words,  $\tilde{I}(\omega)$  is the absorption coefficient normalized to that for graphene without Rashba interaction.

Now, let us define the spin injection rate for the  $i$ -th component of the spin density. Following Eq. (6), we write

$$\begin{aligned} J_i^{n \rightarrow n'}(\omega) &= \frac{2\pi}{\hbar} \int \frac{d^2\mathbf{k}}{(2\pi)^2} \left| \langle \Psi_{n\mathbf{k}} | \hat{H}_A | \Psi_{n'\mathbf{k}} \rangle \right|^2 \\ &\times (\langle \Psi_{n'\mathbf{k}} | \sigma_i | \Psi_{n'\mathbf{k}} \rangle - \langle \Psi_{n\mathbf{k}} | \sigma_i | \Psi_{n\mathbf{k}} \rangle) \\ &\times \delta(E_{n\mathbf{k}} + \hbar\omega - E_{n'\mathbf{k}}) f(E_{n\mathbf{k}}) [1 - f(E_{n'\mathbf{k}})]. \end{aligned} \quad (10)$$

Similarly to the case of absorption, we introduce the total spin injection rate as  $J_i(\omega) = \sum_{n,n'} J_i^{n \rightarrow n'}(\omega)$  and write  $J_i(\omega) = I_0 \tilde{J}_i(\omega)$  and  $J_i^{n \rightarrow n'}(\omega) = I_0 \tilde{J}_i^{n \rightarrow n'}(\omega)$ . Thus,  $\tilde{J}_i(\omega)$  and  $\tilde{J}_i^{n \rightarrow n'}(\omega)$  can be considered as normalized to  $I_0$  spin injection rates. Before discussing numerical results based on the above formula, let us discuss briefly physical origin of the spin injection.

In the absence of magnetic field, symmetry of the matrix elements and spin expectation values (as shown in Fig. 1) as well as the independence of energy  $E_{n\mathbf{k}}$  on the momentum orientation lead to zero spin injection rate, as required by the time-reversal symmetry. In an in-plane magnetic field, in turn, each subband is shifted in energy,  $E_{n\mathbf{k}} - E_{n\mathbf{k}}^{(0)} = g \left( \langle \Psi_{n\mathbf{k}}^{(0)} | \boldsymbol{\sigma} | \Psi_{n\mathbf{k}}^{(0)} \rangle \cdot \mathbf{B} \right)$ . As a result, the lines of energy conservation,  $E_{n\mathbf{k}} + \hbar\omega - E_{n'\mathbf{k}} = 0$ , for the transitions changing the electron spin, such as  $1 \rightarrow 3$  and  $2 \rightarrow 4$ , are not simple circles anymore and acquire a distortion of the order of  $(gB/\lambda) \cos \varphi$ , where  $\varphi$  is the angle between  $\mathbf{k}$  and the  $x$ -axis. In addition, the 4-component wave functions are modified in the first order perturbation as

$$\Psi_{n\mathbf{k}} - \Psi_{n\mathbf{k}}^{(0)} = g \sum_{n'} \frac{\langle \Psi_{n'\mathbf{k}}^{(0)} | (\boldsymbol{\sigma} \cdot \mathbf{B}) | \Psi_{n\mathbf{k}}^{(0)} \rangle}{E_{n\mathbf{k}}^{(0)} - E_{n'\mathbf{k}}^{(0)}} \Psi_{n'\mathbf{k}}^{(0)}. \quad (11)$$

Accordingly, expectation values of the spin components  $\langle \Psi_{n\mathbf{k}} | \sigma_i | \Psi_{n\mathbf{k}} \rangle$  and of the interband matrix elements  $\langle \Psi_{n\mathbf{k}} | \hat{H}_A | \Psi_{n'\mathbf{k}} \rangle$  acquire first-order modification in the applied magnetic field, which results in a nonzero spin injection.

### III. INFRARED ABSORPTION AND SPIN INJECTION: NUMERICAL RESULTS

Now we present some numerical results on the absorption of linearly polarized light and the associated spin injection. In our calculations we assumed the temperature  $T = 1$  K.

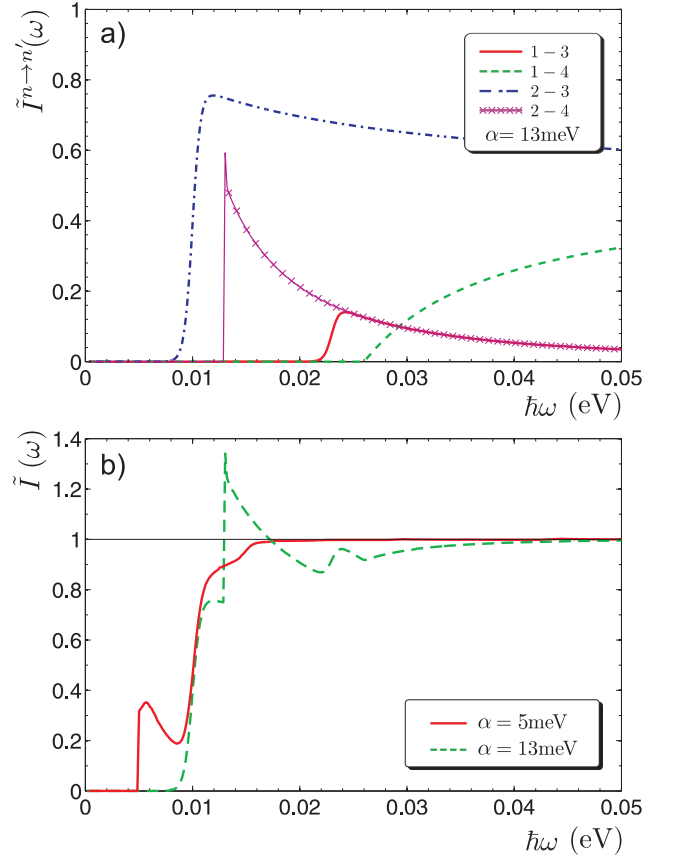


FIG. 2: (Color online). (a) The normalized absorption coefficients corresponding to indicated interband transitions, calculated for  $\alpha = 2\lambda = 13$  meV. (b) The total normalized absorption coefficient for two different values of the Rashba spin-orbit parameter  $\alpha$ , as indicated. Both figures are calculated for magnetic field  $B = 5$  T and for the chemical potential  $\mu = 5$  meV.

Let us begin with the normalized absorption coefficients presented in Fig. 2 as a function of the frequency  $\omega$ . Figure 2a shows the normalized absorption coefficients for individual inter-band transitions, while Fig. 2b shows the total normalized absorption coefficient for two different values of the Rashba parameter  $\alpha$ . In the latter case, the thin solid line corresponds to the absorption

coefficient in the absence of Rashba coupling.

As one can see in Fig. 2, the spin-orbit coupling strongly modifies the absorption, in agreement with the results of Ref. [26]. The frequency threshold for the interband transitions is determined by the Pauli blocking and also depends on the chemical potential  $\mu$  and the spin-orbit splitting  $2\lambda$ . In the case considered here,  $\mu < 2\lambda$ , the transitions of highest frequency occur between the  $n = 1$  and  $n' = 4$  bands and start at the  $K$ -point with zero matrix element. At high frequencies,  $\hbar\omega \gg \lambda$ , the total absorption coefficient approaches that for a pure single-layer graphene without spin-orbit coupling.

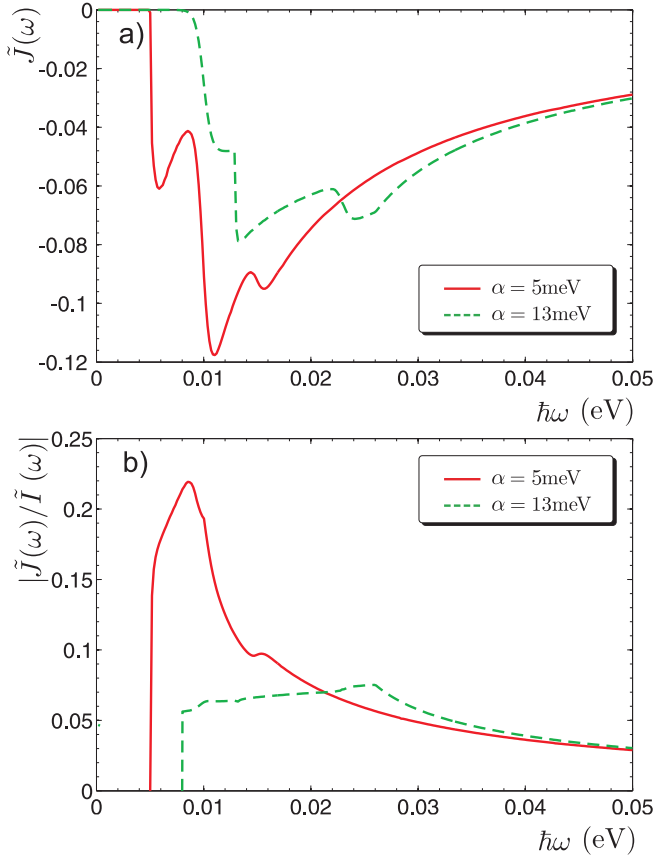


FIG. 3: (Color online). (a) The total injection rate for the spin component  $\sigma_x$  in a magnetic field of  $B = 5 \text{ T}$  parallel to the  $x$ -axis and external electromagnetic field polarized along the  $y$ -axis. The dashed green (solid red) line corresponds to the coupling constant  $\alpha = 2\lambda = 13 \text{ meV}$  ( $\alpha = 2\lambda = 5 \text{ meV}$ ). All results are for the chemical potential  $\mu = 5 \text{ meV}$ . (b) Spin injection efficiency for spin change per absorbed photon for the same parameters and injection geometry.

Let us consider now numerical results on spin injection shown in Fig. 3 for the magnetic field  $B = 5 \text{ T}$ , which corresponds to the Zeeman splitting  $2gB$  of approximately  $0.6 \text{ meV}$ . We show there only the injection rate for the spin  $x$ -component, and for clarity we simplified there the notation by omitting the index  $i$ ,  $\tilde{J}_x(\omega) \equiv \tilde{J}(\omega)$ . Fig-

ure 3a shows the total normalized spin injection rate as a function of frequency for two different values of the Rashba coupling parameter. The dependence of the spin injection rate on the light frequency is rather complicated due to several interband transitions involved and complex dependence of the matrix elements on the transition frequency. For the spin-conserving transitions between the states characterized by the same  $\xi$  in Eq. (3), such as  $1 \rightarrow 4$  and  $2 \rightarrow 3$ , the main contribution to the spin injection comes from changes in the expectation values of  $\langle \Psi_{nk} | \sigma | \Psi_{nk} \rangle$ , while for the other transitions all the changes in the system make comparable contributions. Note, the spin injected is opposite to the magnetic field.

The spin injection efficiency can be defined as the average spin injected by a single photon. This efficiency is given by  $|\tilde{J}(\omega)/\tilde{I}(\omega)|$ , and is shown in Fig. 3b for the same Rashba parameters as in Fig. 3a. As one can see in Fig. 3b, the efficiency can reach 0.2 per incident photon. In general, the injection rate is of the order of  $gB/\lambda$ , and can be manipulated by changing the photon frequency in the range of the order of  $\lambda$ . Since the transitions are rather complicated, the ratio  $gB/\lambda$  should be considered as an order-of-magnitude estimate only.

Similar spin injection, though considerably weaker, can be obtained for the electric field along the magnetic field, i.e. along the  $x$ -axis.

#### IV. SUMMARY AND CONCLUSIONS

We have considered theoretically spin injection in single-layer graphene in the presence of Rashba spin-orbit coupling and in-plane external magnetic field. We have found that the spin injection is efficient at frequencies of the order of spin-orbit band splitting, with the efficiency being of the order of the ratio of Zeeman and Rashba splittings.

For experimentally achievable parameters of the spin-orbit coupling and magnetic field, the injection efficiency can achieve 0.2 per absorbed photon. This result shows that optical spin injection opens a way for a controllable and efficient method of spin density and spin current generation in graphene, not requiring presence of any ferromagnetic contact.

#### Acknowledgements

This work is partly supported by the National Science Center in Poland as a research project in years 2011 – 2014 and Grants Nos. DEC-2011/01/N/ST3/00394 and DEC-2012/06/M/ST3/00042. The work of EYS was supported by the University of Basque Country UPV/EHU under program UFI 11/55, Spanish MEC (FIS2012-36673-C03-01), and "Grupos Consolidados UPV/EHU del Gobierno Vasco" (IT-472-10).

- 
- <sup>1</sup> K. S. Novoselov, A. K. Geim, S. V. Morozov, D. Jiang, M. I. Katsnelson, I. V. Grigorieva, S. V. Dubonos, and A. A. Firsov, *Nature* **438**, 197 (2005).
  - <sup>2</sup> Y. Zhang, Y. W. Tan, H. L. Stormer, and P. Kim, *Nature* **438**, 201 (2005).
  - <sup>3</sup> M. I. Katsnelson, *Graphene: Carbon in Two Dimensions* (Cambridge Univ. Press, 2012).
  - <sup>4</sup> D. L. Nika and A. A. Balandin, *J. Phys.: Condens. Matter* **24**, 233203 (2012).
  - <sup>5</sup> A. R. Ranjbari, B. Wang, X. Shen, and G. Wang, *J. Appl. Phys.* **109**, 014306 (2011).
  - <sup>6</sup> H. Chen, M. B. Møller, K. J. Gilmore, G. G. Wallace, and D. Li, *Adv. Mater.* **20**, 3557 (2008).
  - <sup>7</sup> L. A. Falkovsky, *J. Phys.: Conf. Ser.* **129**, 012004 (2008).
  - <sup>8</sup> F. Bonaccorso, Z. Sun, T. Hasan, and A. C. Ferrari, *Nature Photonics* **4**, 611 (2010).
  - <sup>9</sup> F. S. M. Guimarães, A. T. Costa, R. B. Muniz, and M. S. Ferreira, *Phys. Rev. B* **81**, 233402 (2010).
  - <sup>10</sup> Y. S. Dedkov, M. Fonin, U. Rüdiger, and C. Laubschat, *Phys. Rev. Lett.* **100**, 107602 (2008).
  - <sup>11</sup> A. Varykhalov, J. Sánchez-Barriga, A. M. Shikin, C. Biswas, E. Vescovo, A. Rybkin, D. Marchenko, and O. Rader, *Phys. Rev. Lett.* **101**, 157601 (2008).
  - <sup>12</sup> N. Tombros, C. Jozsa, M. Popinciuc, H. T. Jonkman, and B. J. van Wees, *Nature* **448**, 571 (2007).
  - <sup>13</sup> Wei Han and R. K. Kawakami, *Phys. Rev. Lett.* **107**, 047207 (2011).
  - <sup>14</sup> T. Y. Yang, J. Balakrishnan, F. Volmer, A. Avsar, M. Jaiswal, J. Samm, S. R. Ali, A. Pachoud, M. Zeng, M. Popinciuc, G. Güntherodt, B. Beschoten, and B. Özyilmaz, *Phys. Rev. Lett.* **107**, 047206 (2011).
  - <sup>15</sup> V. K. Dugaev, E. Ya. Sherman, and J. Barnaś, *Phys. Rev. B* **83**, 085306 (2011).
  - <sup>16</sup> L. Wang and M. W. Wu, *Phys. Rev. B* **87**, 205416 (2013); P. Zhang, Y. Zhou and M. W. Wu, *J. Appl. Phys.* **112**, 073709 (2012).
  - <sup>17</sup> D. V. Fedorov, M. Gradhand, S. Ostanin, I. V. Maznichenko, A. Ernst, J. Fabian, and I. Mertig, *Phys. Rev. Lett.* **110**, 156602 (2013), S. Konschuh, M. Gmitra, D. Kochan, and J. Fabian, *Phys. Rev. B* **85**, 115423 (2012).
  - <sup>18</sup> S. Fratini, D. Gosálbez-Martínez, P. M. Cámara, and J. Fernández-Rossier, *Phys. Rev. B* **88**, 115426 (2013).
  - <sup>19</sup> H. Ochoa, A. H. Castro Neto, and F. Guinea, *Phys. Rev. Lett.* **108**, 206808 (2012).
  - <sup>20</sup> M. Ezawa, *Physica E* **42**, 703 (2010).
  - <sup>21</sup> R. P. Tiwari and M. Blaauw, *Appl. Phys. Lett.* **97**, 243112 (2010).
  - <sup>22</sup> Q. Zhang, K. S. Chan, and Z. Lin, *Appl. Phys. Lett.* **98**, 032106 (2011).
  - <sup>23</sup> D. Greenbaum, S. Das, G. Schwiete, and P. G. Silvestrov, *Phys. Rev. Lett.* **75**, 195437 (2007).
  - <sup>24</sup> J. F. Liu and K. S. Chan, *Nanotechnology* **22**, 395201 (2011).
  - <sup>25</sup> *Spin Physics in Semiconductors* (Springer Series in Solid-State Sciences) by M.I. Dyakonov (Berlin, 2008)
  - <sup>26</sup> P. Ingenhoven, J. Z. Bernád, U. Zülicke, and R. Egger, *Phys. Rev. B* **81**, 035421 (2010).
  - <sup>27</sup> E. I. Rashba, *Phys. Rev. B* **79**, 161409 (2009).
  - <sup>28</sup> C. L. Kane and E. J. Mele, *Phys. Rev. Lett.* **95**, 226801 (2005).
  - <sup>29</sup> V. P. Gusynin and S. G. Sharapov, *Phys. Rev. B* **73**, 245411 (2006).
  - <sup>30</sup> A. B. Kuzmenko, E. van Heumen, F. Carbone, and D. van der Marel, *Phys. Rev. Lett.* **100**, 117401 (2008).